

Ambient Pressure Synthesis of Corundum-Type In_2O_3

Mauro Epifani and Pietro Siciliano

Istituto per la Microelettronica e i Microsistemi, IMM-CNR, Sezione di Lecce, Via Arnesano, 73100 Lecce, Italy

Alexander Gurlo,* Nicolae Barsan, and Udo Weimar

Institute of Physical and Theoretical Chemistry, University of Tübingen, Auf der Morgenstelle 8, 72076 Tübingen, Germany

Received December 18, 2003; E-mail: alexander.gurlo@ipc.uni-tuebingen.de

Indium oxide (In_2O_3), which is an n-type semiconductor, is of interest for many device applications and fundamental research, especially due to its high electrical conductivity and high transparency to light.¹ One of the most important and rapidly growing topics currently applied to In_2O_3 is the search for new synthetic strategies to achieve metastable In_2O_3 structures, such as nanofibers and nanowires,^{1a-f} aggregates of nano- In_2O_3 ,^{1g,h} and high-pressure modification of In_2O_3 (corundum-type or hexagonal In_2O_3).^{1f,h,i} Under normal conditions In_2O_3 crystallizes in cubic bixbyite-type structure (cubic- In_2O_3 , space group $Ia\bar{3}$, the cell contains 16 units, denoted as C- In_2O_3 hereafter) (Table 1). Corundum-type indium (III) oxide (hexagonal- In_2O_3 , space group $R\bar{3}c$, the cell contains six formula units, denoted as H- In_2O_3 hereafter) is known to be the high-pressure modification of In_2O_3 .

The novelty of the present study is related to the new synthetic strategy to obtain pure metastable H- In_2O_3 by a simple sol-gel precipitation method under ambient pressure as well as to the general understanding of phase transitions in In_2O_3 .

C- In_2O_3 can be described as an oxygen-deficient fluorite structure with twice the unit-cell edge of the corresponding fluorite cell and with one-quarter of the anions missing in an ordered way. The In^{3+} ions in C- In_2O_3 are of two types. Instead of eight neighbors at the vertexes of a cube, two are missing. For one-quarter of the M atoms these two are at the ends of a body-diagonal ($\text{In}_{\text{In,bd}}^+$) and for the remaining ones, at the ends of a face-diagonal ($\text{In}_{\text{In,fd}}^+$). Both coordination groups may be described as distorted octahedra. Cations of H- In_2O_3 are in a rather regular octahedron. In H- In_2O_3 the In^{3+} ions are distributed in an ordered fashion over two-thirds of the octahedral sites within a framework of hexagonally close-packed O^{2-} ions. The indium-oxygen distances are nearly identical in the two structures. The densities are similar, and the difference is supposed to result from better packing of the anion layers in the H- In_2O_3 modification. In both the C- In_2O_3 and H- In_2O_3 structures the indium-cations are six-coordinated, and the oxygen-anions are four-coordinated.

The cubic to hexagonal phase transition under ambient conditions is supposed to be favored when a foreign atom M with a smaller ionic radius than that of indium is inserted into the cubic indium oxide network. This transition was observed in SnO_2 - In_2O_3 oxides⁶ formed by wet chemical route (coprecipitation, sol-gel technique, hydrothermal treatment) and in In_2O_3 - Fe_2O_3 coprecipitates.¹ⁱ

In this communication, we describe the ambient-pressure synthesis of corundum-type indium oxide by a modified nonalkoxide sol-gel method which allows obtaining pure undoped H- In_2O_3 . The resulting powders as well as films are expected to have potential in solar energy conversions, catalysis, and gas sensors.^{1,6g,7}

For comparison, three series of samples which differ in the solvent (water or methanol) and additive (with or without acetyl-

Table 1. Structural Parameters for Known In-O Phases (adapted from refs 2-5)

phase	space group	Z	cell parameters, Å	$D(\text{In-O})$, Å	d , g/cm ³
C- In_2O_3	$Ia\bar{3}$	16	$a = 10.12$	2.13, 2.19, 2.23, 2.18	7.1
H- In_2O_3	$R\bar{3}c$	6	$a = 5.49; c = 14.52$	2.27, 2.07	7.3
$\text{In}(\text{OH})_3$	$Im\bar{3}$	8	$a = 7.98$	2.17	4.3
InOOH	$Pnmm$	2	$a = 5.16, b = 4.56, c = 3.87$	2.15, 2.20	6.25

acetone) have been synthesized. All the precipitations were carried out at room temperature and under ambient pressure.

The samples in the methanol-based and in the water-based routes were prepared by dissolving 1 g of $\text{In}(\text{NO}_3)_3 \times 5\text{H}_2\text{O}$ in 10 mL of methanol (Aldrich, ACS reagent) or deionized water, respectively and then adding a concentrated (30 wt % in water) ammonia solution to get a NH_3/In molar ratio of 8. The white precipitate was collected by centrifugation (4500 rpm for 10 min), then dried at 80 °C for 40 h. The product was ground and heated at various temperatures in an electrically heated furnace (Thermolyne, 5 °C/min, heating time 1 h). After the heat treatment, the oven was cooled at a rate of 250 °C/h.

The samples in the acetylacetone/methanol-based route (this route was originally conceived for overcoming the uniformity problem in the deposition of thin films encountered when using the sol obtained from peptization-precipitation, ref 8) were prepared by dissolving 1 g of $\text{In}(\text{NO}_3)_3 \times 5\text{H}_2\text{O}$ in 10 mL of methanol. Then acetylacetone (Acros Organics, ACS reagent) was added to get an acacH/In molar ratio of 3; 30 min after the addition of acetylacetone a concentrated (30 wt % in water) ammonia solution was added to get a NH_3/In molar ratio of 2. The resulting sol was dried in a rotary evaporator (Büchi) at 70 °C and reduced pressure (50 mbar) until a powder was obtained. The powder was heated at about 200 °C until the indium acetylacetonato complex contained in the product decomposed; the charred residuals were then heated at different temperatures in a tubular oven in oxygen flow (30 mL/min) (Linn High Therm, heating conditions as above for the other samples). The complex decomposition is strongly exothermic and should be carried out under a hood with proper shielding.

The as-obtained and calcinated powders were characterized by X-ray diffraction (XRD, Philips 1880 diffractometer, $\text{Cu K}\alpha$ radiation) and by scanning electron microscopy (SEM, Zeiss DSM 962 microscope).

Using methanol or H_2O as the solvent does not result in different phases in the starting product; in both cases the phase of the product dried at 80 °C is the indium hydroxide. The stabilization with acetylacetone results in a peculiar phase, which remains unidentified (it may consist of polynuclear species resulting from partial hydrolysis and condensation of hydroxo-acetylacetonato In^{3+}

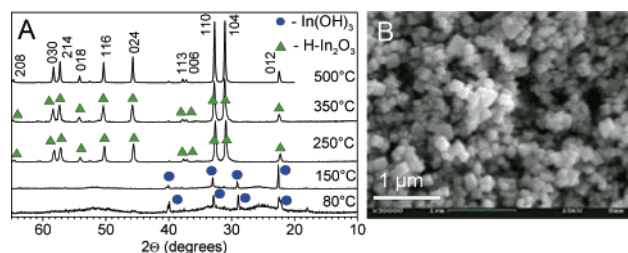


Figure 1. (A) X-ray powder diffraction pattern recorded from the powders prepared in the methanol-based route. For the powders calcined at 250–500 °C, all the peaks can be indexed to H-In₂O₃ with corundum structure (JCPDS 22-336). (B) SEM of the powder prepared in the methanol-based route after calcination at 500 °C.

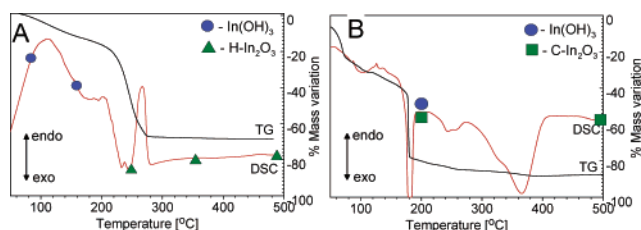


Figure 2. Results of the thermal analysis of the powders prepared in the methanol-based route (A) and acetylaceton/methanol-based route (B). Symbols (circles, cubes, and triangles) denote the phase composition according to the XRD results.

complexes, see Supporting Information). The powder prepared in the methanol-based route becomes H-In₂O₃ after calcination at 250 °C (Figure 1A), while that prepared in water-based route becomes C-In₂O₃. The powder prepared in the acetylaceton/methanol-based route is C-In₂O₃ already after the complex decomposition at 200 °C. The SEM image indicates that H-In₂O₃ consists of cubically shaped grains (Figure 1B).

As shown by thermal analysis (Figure 2), the powders in the acetylaceton/methanol-based route, during the pyrolysis at 200 °C, go through a strongly exothermic process; thus, it is possible that the energy generated in the decomposition vaporizes all the solvents simultaneously, favoring an arrangement of the structure toward the more stable cubic phase. The powders in the methanol-based route, instead, have a behavior similar to those of the water-based route, but there is a critical temperature through which a phase transition occurs from the initial phase—In(OH)₃—which is common to the two processes, to the hexagonal phase, while this does not occur in the powders from the water-based route.

The endothermic peak in the methanol-based route at about 270 °C can be attributed to the pyrolysis of residual ammonium and nitrate ions, as well as to the desorption of residual solvent. It is not clear what causes the difference in the phase composition in the water- and methanol-based routes. By now, we can only speculate that the presence of methanol residuals favors a transition coordination sphere of the In³⁺ ions that can evolve to the hexagonal phase. On the other hand, chelating agent (acetylaceton) not only permits control of the reactivity by avoiding fast hydrolysis and condensation of the precursor in contact with ammonia–water solution but also influences the phase composition of the obtained precipitate.⁸

Another point which we have to keep in mind is that the stabilization of H-In₂O₃ under ambient conditions (in fact, synthesis under ambient pressure) was observed for both undoped and doped

(with Sn, Fe) In₂O₃ structures prepared either by sol–gel method or coprecipitation. Both of these methods involve most obviously the formation of H-In₂O₃ via the phase transformation of In(OH)₃ (either pure or doped). Therefore, the structure of the initial precipitate, which includes either metal cations (for example, Sn⁴⁺, $r = 83$ pm in octahedral coordination; Fe²⁺, $r = 92$ pm in octahedral coordination and high spin configuration, cited from ref 9) smaller than In³⁺ ($r = 94$ pm in octahedral coordination) or anions or organic molecules (for example, NO₃[−], $r = 165$ pm) larger than O^{2−} ($r = 124$ pm in tetrahedral coordination), plays the crucial role in the formation of H-In₂O₃. As shown in ref 10, both structures—In(OH)₃ (collapsed perovskite structure, $\square^A\square_3^A\text{In}_4(\text{OH})_{12}$, space group *Im*3) and H-In₂O₃ (collapsed perovskite structure ABX₃, space group $R\bar{3}c$)—are topologically related to the perovskite structure and can be easily transformed into one another. This transformation involves most obviously a change in unit-cell shape and some anion shifts. The small cations as well as large anions favor the transformation of indium hydroxide into H-In₂O₃.

In summary, we have demonstrated the large-scale synthesis of the metastable indium oxide with corundum structure under ambient pressure.

Acknowledgment. This work was supported in the frame of the INCO Copernicus GASMOH (ICA2-CT-2000-10041) project.

Supporting Information Available: X-ray powder diffraction pattern recorded from the powders prepared in acetylaceton/methanol-based route; SEM image of the powder prepared in acetylaceton–methanol-based route (PDF). This material is available free of charge via the Internet at <http://pubs.acs.org>.

References

- (1) (a) Zhang, D. H.; Li, C.; Han, S.; Tang, T.; Zhou, C. *Appl. Phys. Lett.* **2003**, *83*, 1845. (b) Li, C.; Zhang, D. H.; Han, S.; Liu, X. L.; Tang, T.; Zhou, C. *Adv. Mater.* **2003**, *15*, 143. (c) Zhang, J.; Qing, X.; Jiang, F.; Dai, Z. *Chem. Phys. Lett.* **2003**, *371*, 311. (d) Li, Y.; Bando, Y.; Golberg, D. *Adv. Mater.* **2003**, *15*, 581. (e) Li, C.; Zhang, D. H.; Liu, X. L.; Han, S.; Tang, T.; Han, J.; Zhou, C. *Appl. Phys. Lett.* **2003**, *82*, 1613. (f) Yu, D.; Yu, S. H.; Zhang, S.; Zuo, J.; Wang, D.; Qian, Y. *Adv. Funct. Mater.* **2003**, *13*, 497. (g) Soullantica, K.; Erades, L.; Sauvan, M.; Senocq, F.; Maisonnat, A.; Chaudret, B. *Adv. Funct. Mater.* **2003**, *13*, 553. (h) Gurlo, A.; Barsan, N.; Weimar, U.; Ivanovskaya, M.; Taurino, A.; Siciliano, P. *Chem. Mater.* **2003**, *15*, 4377. (i) Gurlo, A.; Ivanovskaya, M.; Barsan, N.; Weimar, U. *Inorg. Chem. Commun.* **2003**, *6*, 569.
- (2) Marezio, M. *Acta Crystallogr.* **1969**, *20*, 723.
- (3) Prewitt, C. T.; Shannon, R. D.; Rogers, D. B.; Sleight, A. W. *Inorg. Chem.* **1969**, *8*, 1985.
- (4) Christensen, A. N.; Broch, N. C.; Heidenstam, O.; Nilsson, A. *Acta Chem. Scand.* **1967**, *21*, 1046.
- (5) Christensen, A. N.; Gronbek, R.; Rasmussen, S. E. *Acta Chem. Scand.* **1964**, *18*, 1261.
- (6) (a) Yu, D.; Wang, D.; Lu, J.; Qian, Y. *Inorg. Chem. Commun.* **2002**, *5*, 475. (b) Frank, G.; Olazcuaga, R.; Rabenau, A. *Inorg. Chem.* **1977**, *16*, 1251. (c) Kim, B.-C.; Kim, J.-J.; Chang, S.-H. *Mater. Res. Soc. Symp. Proc.* **2000**, *581*, 27. (d) Parent, Ph.; Dexpert, H.; Tourillon, G.; Grimal, J.-M. *J. Electrochem. Soc.* **1992**, *139*, 276. (e) Malik, A.; Nunes, R.; Martins, R. *Mater. Res. Soc. Symp. Proc.* **1998**, *481*, 599. (f) Coutal, C.; Azema, A. Roustan, J.-C. *Thin Solid Films.* **1996**, *288*, 248. (g) (c) Kim, B.-C.; Kim, J.-J.; Lee, D.-D.; Lim, J.-O.; Huh, J.-S. *Sens. Actuators B.* **2003**, *89*, 180.
- (7) Gurlo, A.; Barsan, N.; Ivanovskaya, M.; Weimar, U.; Göpel, W. *Sens. Actuators B.* **1998**, *47*, 327.
- (8) Epifani, M.; Capone, S.; Rella, R.; Siciliano, P.; Vasanelli, L.; Faglia, G.; Nelli, P.; Sberveglieri, G. *J. Sol-Gel. Sci. Technol.* **2003**, *26*, 741.
- (9) Huheey, J.; Keiter, E.; Keiter, R. *Inorganic Chemistry. Principles of Structure and Reactivity*; Harper Collins: New York, 1993.
- (10) Hyde, B. G.; Andersson, S. *Inorganic Crystal Structures*; Wiley & Sons: New York, 1989; p 299.

JA0318075